THE ASTROPHYSICAL JOURNAL, 356:49–56, 1990 June 10

ANTIPODAL MICROWAVE

RUTH DURRER AND ISRAEL KOVNER[1]
Institute of Astronomy, Madingley Road, Cambridge, United Kingdom
Received 1989 August 17; accepted 1989 December 14

ABSTRACT

We examine inflectional Friedmann-Lemaître universes and find that current observations (gravitational lenses and QSO absorption lines) cannot rule out an antipode at $z_a > 5$. For $z_a \gg 1$, the structure on the recombination shell is magnified, and the linear size observed at a given angular scale is much smaller than in an Einstein–de Sitter universe. In the extreme case of an antipode near or inside the shell, $|z_a - z_r| \lesssim \Delta z_r$, the (linear) magnification is $M_a \sim 800\Omega_{m0}^{1/2}$; thus $\delta T/T$ is reduced by photon diffusion and projection effects on scales $\lesssim 90°$ (rather than $\lesssim 8'$ in an Einstein–de Sitter universe). If $250 < z_a < \infty$, we observe the microwave background radiation (MBR) emitted within a causally connected region; thus anisotropies from the Sachs-Wolfe effect are reduced.

A high-redshift antipode produces anomalous ratios between the coefficients of the Taylor expansion of the MBR autocorrelation function. It can thus be ruled out or discovered when two or more such coefficients are measured. A simple test is the decrease of multibeam anisotropy measurements with the number of beams, on angular scales within some range above $8' \times \Omega_{m0}^{-1/2}$ (in contrast to predictions of various theories in a flat universe).

In addition, gravitational lensing by galaxies and clusters reduces MBR brightness contrasts on scales $\lesssim 1'$–$1°$. To our knowledge, this effect has not been correctly appreciated before. We point out that it is analogous to the reflection of the Sun in an undulating water surface. However, on these scales, the antipodal magnification and the damping already reduce $\delta T/T$ below the present-day sensitivity. Thus lensing by galaxies and clusters is irrelevant for current bounds on the MBR anisotropy (as it is in conventional cosmologies).

An antipode at $z_a \sim 5$–10 may produce a departure of the MBR from the blackbody spectrum, if it lies inside an infrared source. An obvious prediction, then, is large dipole and higher multipole moments of the departure, with axes uncorrelated with the known MBR dipole.

Subject headings: cosmic background radiation — cosmology — gravitational lenses

I. INTRODUCTION

The microwave background radiation (MBR) is very homogeneous, and recent observational bounds on its anisotropy severely constrain current theories of galaxy formation (e.g., Davies 1988; Efstathiou and Bond 1987; Silk and Vittorio 1987). In this paper we present a scarcely explored possibility which may reduce the connection between the observed structure in the universe and the high isotropy of the MBR.

This reduction is due to cooperation of two effects: the damping of the brightness fluctuations on scales smaller than the MBR shell thickness and the large magnification of these scales by the curvature of the universe which creates or almost creates a real image of a small patch of the MBR shell around us. The damping is caused by photon diffusion (Peebles 1980, § 92C and references therein) and by cancellation of wave trains in projection (for Gaussian perturbations; the same as considered by Kaiser 1984 for reionization).

Suppose that we live in a closed ($k = +1$) Friedmann-Lemaître universe, and the cosmological constant ($\Lambda > 0$) is such that we have an antipode at a redshift $z_a \gg 1$. Then we see the structure of the MBR shell magnified, as compared with the standard cosmographies. In particular, the scale of a few arcminutes or degrees can correspond to linear sizes much smaller than the MBR shell thickness. The magnification and the damping reduce the theoretical predictions for brightness fluctuations, by up to several orders of magnitude.

In addition, if $z_a \gtrsim 250$ all the MBR observed in the whole sky comes from a causally connected region which is comparable in size to observed voids in the galaxy distribution ($\sim$10–100 Mpc). The causal connection also reduces the Sachs-Wolfe effect (Sachs and Wolfe 1977). These possibilities are relevant for the MBR quadrupole and the lower multipoles which are not reduced by the magnification-damping combination.

The effect of magnification has been noticed earlier by Blanchard (1984); however, he did not investigate the observational constraints on such a possibility, the variety of effects produced by antipodes, and possible tests for these effects.

Before exploring our proposition, let us recall that various observational constraints exclude a very large vacuum energy density: in five out of six combinations of k and sign Λ ($k = 0, \pm 1$ for $\Lambda < 0$, and $k = 0, -1$ for $\Lambda > 0$), the present value of $|\Omega_{v0}| \equiv |\Lambda|/3H_0^2$ is constrained by $|\Omega_{v0}| <$ a few times Ω_{m0}, where $\Omega_{m0} \equiv (8\pi G/3H_0^2)\rho_m(t_0)$ denotes the present matter density parameter (cf. recent review by Weinberg 1989, and references therein). The otherwise weak upper limits on $\Lambda > 0$ can be improved by arguments based on restrictions from the MBR isotropy on the structure formation (Durrer and Straumann 1990). Clearly, a vacuum energy density $\Omega_{v0} \lesssim \Omega_{m0}$ cannot have severe implications for the history of the universe, up to the present.

In the remaining case ($k = +1, \Lambda > 0$), the necessity of a big bang to produce the MBR further restricts the cosmological constant $\Lambda < \Lambda_{crit}(\Omega_{m0})$, in excluding the bouncing universe

1 Also Physics Department, Weizmann Institute, Rehovot 76100, Israel; Incumbent of the Charles H. Revson Foundation Career Development Chair.

with a maximal redshift and no big bang. (Recently Ehlers and Rindler 1989 derived the same limit for all reasonable values of Ω_{m0} without referring to the nature of the MBR.)

The combination $k = +1$ and $0 < \Lambda_{\rm clos}(\Omega_{m0}) < \Lambda < \Lambda_{\rm crit}(\Omega_{m0})$ leads to an inflectional universe, which we consider in this paper. In this universe the expansion first decelerates until some redshift z_i, and then accelerates. $\Lambda = \Lambda_{\rm crit}$ is the boundary between inflectional and bouncing universes. $\Lambda > \Lambda_{\rm clos}$ guarantees that the universe is closed. If the loitering phase ($z \sim z_i$) is long enough, the inflectional universe exhibits one or more antipodes. Petrosian, Salpeter, and Szekeres (1967), Shklovsky (1967), and Rowan-Robinson (1968) investigated extreme loitering at redshifts ~ 2. More recently, Gott (1985), Gott and Rees (1987), and Gott, Park, and Lee (1989) revived the subject by seeking constraints on redshifts of antipodes from gravitational lensing.

In § II we outline a convenient description of the expansion dynamics. In § III we examine observable properties in which a loitering universe with an antipode may differ from an Einstein–de Sitter universe. In § IV we explore effects produced by high-redshift antipodes: The possible causal connection of the MBR shell, reduction of theoretical predictions for the MBR anisotropy from a combination of magnification and damping, departure from the blackbody spectrum which may be produced by a moderately high-redshift antipode. In particular, we outline how a high-redshift antipode can be ruled out or discovered. In § V we investigate the redistribution of MBR brightness due to gravitational lensing by galaxies and clusters. We state and discuss our conclusions in § VI.

II. EXPANSION OF THE UNIVERSE AND ANTIPODES

In this section we describe the expansion of a closed universe with $\Lambda > 0$, in a way convenient for the investigation of antipodes.

a) Expansion Dynamics

The Robertson-Walker metric of a closed universe can be written as

$$ds^2 = a^2(\eta)[-d\eta^2 + d\chi^2 + \sin^2 \chi(d\theta^2 + \sin^2 \theta \, d\phi^2)] \, , \quad (2.1)$$

where η denotes conformal time ($\eta = \eta_0$ at present, and $\eta = 0$ at the big bang). We consider a postrecombination universe dominated by nonrelativistic matter and vacuum energy and governed by the Friedmann-Lemaître equation,

$$(\dot{a}/a)^2 + 1 = (aH)^2(\Omega_v + \Omega_m) \, , \quad (2.2)$$

where $\dot{a} \equiv da/d\eta$. The Hubble rate is $H = \dot{a}/a^2$, and the energy densities in units of the closure density are $\Omega_v = \Lambda/3H^2$ for vacuum, and $\Omega_m = 8\pi G\rho_m/3H^2$ for nonrelativistic matter (the speed of light is $c = 1$).

We represent the evolution of the scale factor of the universe as a particle motion in a potential, which is *harmonic* for $\Lambda = 0$. That is,

$$4\dot{b}^2 + b^2 - k_v b^6 = k_m \, , \quad (2.3)$$

where

$$b = \left(\frac{a}{a_0}\right)^{1/2} = \frac{1}{(1+z)^{1/2}} \, , \quad (2.4)$$

$$k_v = \frac{\Lambda a_0^2}{3} = \frac{\Omega_{v0}}{\Omega_{v0} + \Omega_{m0} - 1} \, ,$$

$$k_m = \frac{8\pi G\rho_{m0} a_0^2}{3} = \frac{\Omega_{m0}}{\Omega_{v0} + \Omega_{m0} - 1} \, , \quad (2.5)$$

and z is the redshift. The conformal time-redshift relation is given by

$$\eta(b) = \eta_0 - 2\int_{bk_m^{-1/2}}^{k_m^{-1/2}} (1 - x^2 + k_v k_m^2 x^6)^{1/2} \, dx \, . \quad (2.6)$$

(Note that the integral [2.6] remains finite in the limit $b \to \infty$, and thus the *conformal* time of the inflectional universe is bounded from above.) The universe started at $b = 0$ and $\eta = 0$ (the initial singularity, big bang), whereas $b = 1$ and $\eta = \eta_0$ at present.

The effective potential,

$$V(b) = b^2 - k_v b^6 \, , \quad (2.7)$$

has a maximum, $V_{\max} = 2/[3(3k_v)^{1/2}]$, at

$$b = b_m = (3k_v)^{-1/4} \, , \quad z_m = (3k_v)^{1/2} - 1 \, . \quad (2.8)$$

We can parameterize the inflectional universe by Ω_{m0} and z_m:

$$\Omega_{v0} = \frac{1 - \Omega_{m0}}{1 - 3(1 + z_m)^{-2}} \, , \quad (2.9)$$

$$V_{\max} = \frac{2}{3(1 + z_m)} \, , \quad (2.10)$$

and

$$k_m = \frac{(1 + z_m)^2 - 3}{3(\Omega_{m0}^{-1} - 1)} \, . \quad (2.11)$$

We consider $\Omega_{m0} < 1$ and only the inflectional universe, $k_m > V_{\max}$, i.e., the maximum of the potential cannot exceed the "energy." Then for fixed Ω_{m0} we see from equations (2.10) and (2.11) that the "loitering" redshift, z_m, is bounded from below by its "critical" value, z_c, in the Eddington-Lemaître ($k_m = V_{\max}$) universe, given by

$$\Omega_{m0} = \frac{2}{z_c^2(3 + z_c)} \, . \quad (2.12)$$

The inversion of equation (2.12), for $\Omega_{m0} \le 0.5$, is given in the Appendix. We also note in the Appendix that the critical redshift, z_c, is an upper bound on the redshift of the inflection, z_i, at which the deceleration parameter changes sign.

We conclude that inflectional universes are possible for Λ in the range given by

$$1 - \Omega_{m0} < \Omega_{v0} < \Omega_{\rm crit}(\Omega_{m0}) = (1 + z_c)^3 \Omega_{m0}/2 \, . \quad (2.13)$$

The last equation is obtained by noting that $\Omega_{v0} = (k_v/k_m)\Omega_{m0}$ and inserting the critical values.

b) Antipodes

We set $\chi_0 = 0$; thus, the first (nearest to us) antipode is (an event) at $(\chi, \eta) = (\pi, \eta_0 - \pi)$. For it to exist, we require $\eta_0 > \pi$. Given Ω_{m0}, this leads to an upper bound on z_m, as indicated in Figure 1.

If $\Lambda = 0$, the dynamics of the universe corresponds to a harmonic oscillator of frequency $\frac{1}{2}$, independent of the "energy," k_m, and it must complete a quarter-period (maximum expansion) of its swing after the big bang, until an antipode shows up. The oscillator is sped up by $\Lambda < 0$, so that an antipode can exist only in the contraction phase. In the opposite case, $\Lambda > 0$, the universe slows down so that an antipode can appear in the expansion phase.

Setting $\eta(b_n) = \eta_0 - n\pi$ determines the redshift of the nth antipode, $z_{an} = b_n^{-2} - 1$ (if it exists at all). Given k_v, the redshift

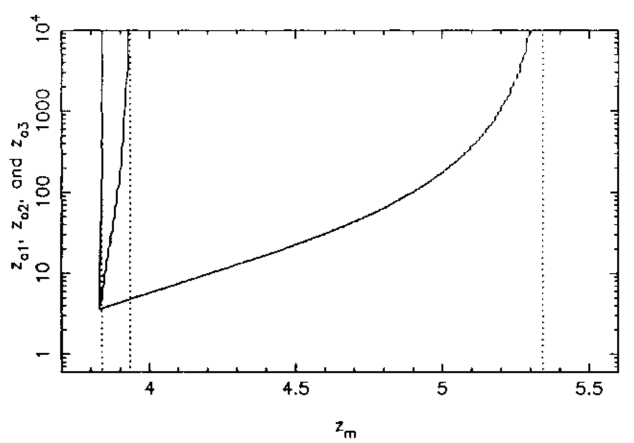

FIG. 1.—Redshifts of the first three antipodes versus the redshift of the maximum of the effective potential (cf. eqs. [2.7] and [2.8]) shown for $\Omega_{m0} = 0.02$. The three limiting values of z_m are 3.84, 3.93, and 5.34, and $z_c = 3.83$. For $z_m > 5.34$ no antipode has yet appeared.

of the first antipode is bounded from below by the redshift, z_{a1c}, of the first antipode in the critical case, $k_m = V_{max}$. In the critical case, an infinite number of antipodes pile up at redshift z_c (cf. the diagrams of Rowan-Robinson 1968). The integral in equation (2.6) is then analytic, with the result

$$\eta[(b(z)] = \eta_0 + \ln\left[\frac{f(z)}{f(0)}\right], \tag{2.14a}$$

where

$$f(z) = 1 + \sqrt{3}\,\frac{\sqrt{3}(2 + z + z_c) + 2[(1 + z_c)(3 + 2z + z_c)]^{1/2}}{z_c - z}. \tag{2.14b}$$

Redshifts of the first three antipodes are plotted against z_m, for $\Omega_{m0} = 0.02$, in Figure 1, and the dependence of z_c and z_{a1c} on Ω_{m0} is shown in Figure 2.

We see that in the case of a pileup of antipodes, the first antipode redshift is very nearly the critical redshift. Therefore z_c is an acccurate approximation for the lower bound on the redshift of an antipode.

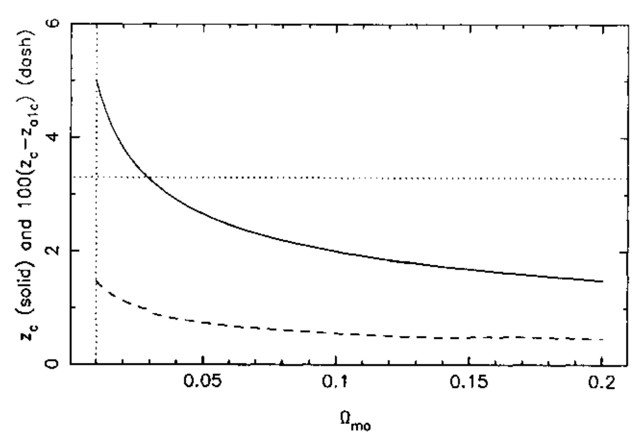

FIG. 2.—Critical redshift z_c and the difference between z_c and the redshift of the 1st antipode, z_{a1c}, in an Eddington-Lemaître universe (multiplied by 100), are plotted against the nonrelativistic matter density Ω_{m0}. The horizontal dotted line indicates the Gott, Park, and Lee (1989) bound on the redshift of an antipode, $z = 3.3$. The vertical dotted line indicates the lower observational bound on Ω_{m0}.

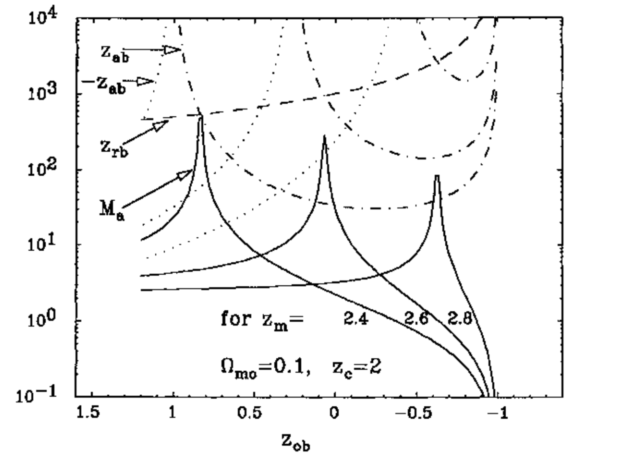

FIG. 3.—Evolution of antipodes. Antipodal (z_{ab}: *dot-dash and dotted curves*) and recombination (z_{rb}: *dashed curves*) redshifts, and the antipodal magnification of the MBR shell (M_a: *solid curves*, as compared with an Einstein–de Sitter universe), from the point of view of an observer at an epoch redshifted by z_{ob} from us ($z_{ob} < 0$ for our descendants).

We note that the redshift of an antipode is time-dependent. Let an observer at an epoch characterized by redshift z_{ob} have an antipode at redshift z_{ab} with respect to the observer, so that this antipode has redshift $z_a = -1 + (1 + z_{ab})(1 + z_{ob})$ with respect to us. We can find z_a by substituting $[k_m(1 + z_{ob})]^{-1/2}$ in the upper limit of the integral in equation (2.6), and solving equation $\eta = \eta_0 - n\pi$. Some examples of $z_{ab} = z_{ab}(z_{ob}, \Omega_{m0}, z_m)$ for the first antipodes of past, present, and future observers are shown in Figure 3. There the cases of "almost antipodes," i.e., small $\pi - \eta_0 > 0$, are also included by setting formally $\eta_a < 0$, $b_a < 0$, and $1 + z_a = -b_a^{-2}$ (*dotted lines*). For analytic estimates from equation (2.6), the Eddington-Lemaître universe provides an upper bound on the variation of the conformal epoch of an antipode with the observer epoch, from equation (2.14).

III. OBSERVATIONAL CONSTRAINTS

In this section we examine observational constraints on loitering and antipodes.

a) Gravitational Lensing and Matter Density Constraints

Gott, Park, and Lee (1989) argue that the redshift of the first antipode is constrained by

$$z_{a1} > z_{min} \approx 3.3 , \tag{3.1}$$

from gravitational lensing effects (or rather their absence). The statistical confidence of their arguments is determined by the number of known high-redshift QSOs (e.g., Hewitt and Burbidge 1987). A conservative lower bound on the density parameter of pressureless matter is given by

$$\Omega_{m0} > 0.01 \tag{3.2}$$

(Trimble 1987). Taking equations (3.1) and (3.2) as fiducial constraints, we find, from the dependence of z_c on Ω_{m0} (cf. Fig. 2), the range of values of the matter density parameter,

$$0.01 \le \Omega_{m0} \le 0.03 , \tag{3.3}$$

for which multiple antipodes are not excluded by gravitational lensing and by nonrelativistic matter density. The present-day uncertainties in Ω_{m0} and z_{min} thus leave open some marginal possibility for multiple antipodes.

b) *Absorption Lines*

The piling up of absorption lines in QSO spectra at the inflection redshift was once a motivation for considering extremely loitering universes (Rowan-Robinson 1968 and references therein). At present, the most numerous statistics of high-redshift objects are provided by Lyα forests in QSO spectra which have been investigated up to $z = 4.1$ (Q0000 − 26 [cf. Webb *et al.* 1988] and the next highest redshift Lyα forest, Q2000 − 330 at $z = 3.75$ [Carswell *et al.* 1987]). The majority of Lyα clouds are optically thin; thus the forest density is affected by the ionizing background as well as by the distribution of properties of clouds.

We illustrate in two examples various possible effects of loitering on Lyα forests. First, let us suppose a long loitering period, a steady population of Lyα clouds with negligible evolution, and a steady population of sources of ionizing radiation, e.g., star-forming galaxies, which turned on at the beginning of loitering or earlier. The Olbers effect (Kovner and Rees 1989) may then enhance the intensity of the ionizing background radiation toward the end of loitering, and thus moderate, or perhaps even invert, the effect of piling up of absorption lines. However, this moderation is valid only for redshifts preceding the end of loitering, since the enhanced ionizing background will propagate to lower redshifts. Therefore there may be a feature, possibly a step up (with increasing z, near z_c) in the redshift distribution of Lyα clouds, $dN(z)/dz$.

On the other hand, the stimulation of density perturbation growth due to loitering (Occhionero *et al.* 1980; see also below) can cause a gradual appearance of most of the ionizing sources and Lyα clouds toward the end of the loitering period. Then, there may be a step down in $dN(z)/dz$.

The logarithmic slope of the density of absorption lines, $\gamma \sim d\ln(dN/dz)/d\ln(1+z)$ (often addressed in analyses of observations), calculated without taking into account their possible evolution and the Olbers effect, is shown in Figure 4 (see also Petrosian, Salpeter, and Szekeres 1967). The logarithmic slopes usually reported are $\gamma \sim 2$–3. These slopes indicate some evolution at $z > 2$; however, it is questionable whether pileup effects or their absence at $z \gtrsim 4$ can be established from the known high-z Lyα forests.

c) *Growth of Density Perturbations*

In the short-wave limit, the equation of growth of $\Delta = \delta\rho/\rho$ for pressureless matter is

$$\ddot{\Delta} + (\dot{a}/a)\dot{\Delta} - 4\pi G\rho a^2\Delta = 0 \qquad (3.4)$$

(Peebles 1980). During a long loitering period ($\dot{a}/a$ small) this leads to a nearly exponential growth with rate $\omega(\Omega_{m0}, z_i)$,

$$\omega^2 \approx 4\pi G\rho a^2(z_i) = \frac{1}{3}\frac{\Omega_{m0}(z_i+1)}{\Omega_{m0}(z_i+1)^3 + 2\Omega_{m0} - 2}\,. \qquad (3.5)$$

After the loitering phase ($z \ll z_i$) there is no growth of density perturbations, since the universe expands exponentially. This means that only perturbations which become nonlinear by the end of the loitering period can develop in such a universe. This leads in a natural way to a scale-dependent bias in structure formation.

The numerical solution of equation (3.4) in several interesting cases (Ω_{m0}, z_a) is shown in Figure 4 and is compared with the linear growth law ($\Delta \propto a$) in an Einstein–de Sitter universe (see also Occhionero *et al.* 1980). From Figure 4 we conclude that the growth of density perturbation in a Friedmann-Lemaître universe with a single antipode at high redshift differs little from the growth in an Einstein–de Sitter universe.

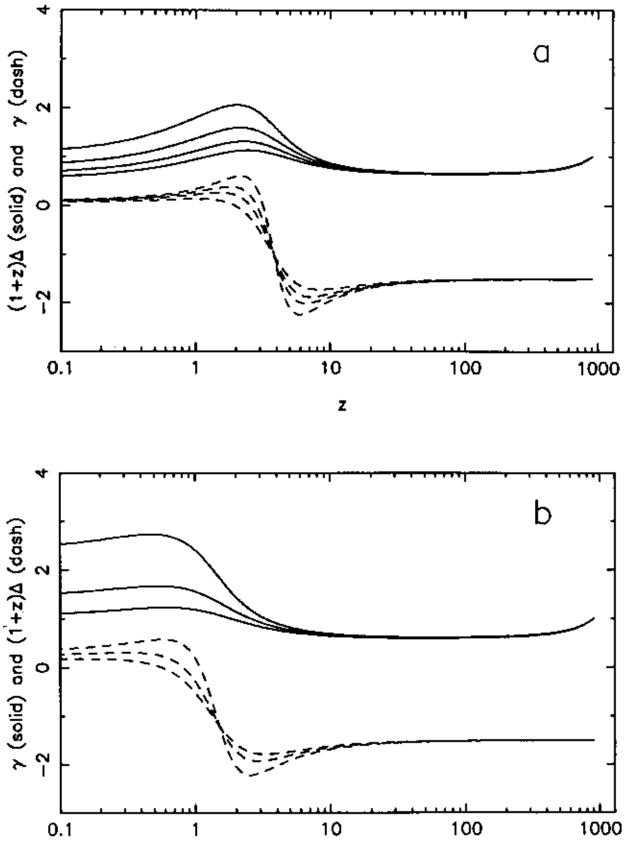

FIG. 4.—Growth of density perturbations compared with the growth in an Einstein–de Sitter universe, $\Delta(z)/\Delta_{\mathrm{EdS}}(z)$. The logarithmic slope, $\gamma = d\ln(dN/dz)/d\ln(1+z)$, of the distribution of absorption lines as a function of redshift in the case of no intrinsic evolution and neglecting the Olbers effect is also presented. The top curves correspond to the lowest values of z_a. (*a*) $\Omega_{m0} = 0.02$, $z_a = 560, 51, 17, 7.3$; (*b*) $\Omega_{m0} = 0.2$, $z_a = 230, 23, 6.6$.

It may be tempting to speculate that some loitering might have stimulated the formation of galaxies at a certain redshift, which led to a burst of massive production of QSOs, at $z \sim 2$. However, we do not examine this possibility in this paper.

IV. HIGH-REDSHIFT ANTIPODES AND MICROWAVE BACKGROUND

Finally, let us consider a single antipode at $z_0 \gg 1$, and its effect on our interpretation of the microwave background radiation.

a) *Causality and Sachs-Wolfe Effect*

If our antipode were exactly at the big bang, $\eta_a = 0$, our past light cone would be a slice of the whole universe, and every event we observed, including the spherical shell which emitted the MBR, would be causally connected with a single event at the big bang, $(\eta, \chi) = (0, \pi)$, on the world line of the antipode. For an antipode at $\eta_a > 0$ the condition that the observed MBR shell is causally connected with event $(\eta, \chi) = (0, \pi)$ is $|\eta_a - \eta_r| \le \eta_r$, where η_r denotes the recombination time. The antipode can be either behind or in front of the MBR shell. The ratio

$$f = |\eta_a - \eta_r|/\eta_r \qquad (4.1)$$

gives the linear fraction of the horizon size at η_r contained in the observed MBR shell. If $z_a \gg 1$ and $z_r \gg 1$, we can approximate $(\eta_a/\eta_r)^2 \approx z_r/z_a$, and find the range of redshifts of an antipode for which $f < f_m$:

$$\frac{1}{(1+f_m)^2} < \frac{z_a}{z_r} < \frac{1}{(1-f_m)^2} \quad \text{for } f_m < 1 \tag{4.2}$$

and

$$\frac{z_a}{z_r} > \frac{1}{(1+f_m)^2} \quad \text{for } f_m \geq 1 \, . \tag{4.3a}$$

The case of an "almost antipode," i.e., $0 < \pi - \eta_0 \ll 1$, produces magnification effects similar to those of an existing high-redshift antipode described in the next subsection. We take this possibility into account by setting formally $\eta_a < 0$, $b_a < 0$, and $z_a \approx -4/k_m \eta_a^2 < 0$ (for $|z_a| \gg 1$). Thus we add the formal inequality

$$\frac{z_a}{z_r} < -\frac{1}{(1-f_m)^2} \quad \text{for } f_m \geq 1 \tag{4.3b}$$

to equation (4.3a).

The MBR was emitted at redshift $z_r \approx 10^3$ within a redshift interval $\Delta z_r \approx 80$ (Jones and Wyse 1985). Hence, in the presence of an antipode at

$$z_a > z_{\min} \approx 250 \, , \tag{4.4}$$

we would observe the microwave background from a volume *causally connected* to at least one single event. The relative importance of the Sachs-Wolfe effect (which dominates MBR anisotropies on scales larger than the horizon size) is thus reduced.

On the other hand, because of the finite thickness of the recombination shell, we observe at least a fraction

$$f_{\min} \sim \Delta z_r/2z_r \sim 0.04 \tag{4.5}$$

of the horizon size. Since the physical thickness of the microwave shell is

$$\Delta l_r \sim 8\Omega_{m0}^{-1/2} h^{-1} \text{ kpc} \, , \tag{4.6}$$

the smallest possible size of the MBR sky would expand by now to $\sim 8\Omega_{m0}^{-1/2}h^{-1}$ Mpc (the horizon size at recombination would expand to $\sim 200\Omega_{m0}^{-1/2}h^{-1}$ Mpc), where $h = H_0/100$ km s^{-1} Mpc^{-1}.

b) Antipodal Magnification of the Damped Anisotropy Scales

Because of the finite time it took the primordial plasma to (re)combine, perturbations on scales smaller than Δl_r are substantially damped (Peebles 1980, § 92C and references therein). In addition, the brightness fluctuations on angular scales smaller than $\Delta\theta_r$ (subtended by Δl_r) are damped by cancellation in projection, for Gaussian perturbations well approximated by coherent wave trains (similar to the effects considered by Kaiser 1984 for reionization). Both the damping mechanisms lead to the typical scaling

$$C^{(n)} \propto \Delta\theta_r^{-n} \tag{4.7}$$

of the coefficients in the Taylor expansion of the brightness autocorrelation function, $C(\theta) = \sum C^{(n)}\theta^n/n!$ If the unperturbed universe is isotropic, $C^{(2m+1)} = 0$. The MBR observations on small angular scales aim to measure $C^{(2)}$ in double-beam experiments, $C^{(4)}$ in triple-beam experiments, and so on (e.g., Bond and Efstathiou 1984). In the usually discussed flat and open universes, $\Delta\theta_r \sim 8' \times \Omega_{m0}^{-1/2}$; thus the damping affects only scales of a few arcminutes and less. In the presence of a high-redshift antipode, these scales can be magnified by 2–3 orders of magnitude.

Since the epoch of an antipode depends on the epoch of observation (cf. Fig. 3), let us consider the "antipodal" magnification from the point of view of an observer at epoch redshifted by z_{ob} from us ($-1 < z_{ob} < 0$ for our descendants). For her the epoch at conformal time η_r is redshifted by $z_{rb} = -1 + (1 + z_r)/(1 + z_{ob})$. If she interprets her observations assuming various cosmologies, the curvature of space of an inflectional universe acts like a magnifying glass, enlarging the angular size of all structure at η_r, by a factor

$$M_a = \frac{d_{os}(k=0, \Lambda=0)}{d_{os}(k=+1, \Lambda=0)} = \frac{2(\Omega_m + \Omega_v - 1)^{1/2}}{|\sin(\eta_r - \eta_a)|}\left[1 - \frac{1}{(1+z_{rb})^{1/2}}\right], \tag{4.8}$$

as compared with an Einstein–de Sitter universe, where we took into account that the angular diameter distances are

$$d_{os}(k=0, \Lambda=0) = (2/H)(1+z_{rb})^{-1}[1-(1+z_{rb})^{-1/2}] \, ,$$

and

$$d_{os}(k=+1, \Lambda>0) = a(1+z_{rb})^{-1}|\sin(\eta_r - \eta_0)| \, .$$

As the MBR shell has a finite thickness given by equation (4.6), the practically observable magnification cannot exceed an upper bound which can be approximated by substitution of Δl_r instead of $d_{os}(k = +1, \Lambda > 0)$ in equation (4.8). At present ($z_{ob} = 0$) for $z_a \gg 1$,

$$M_a \approx \frac{\Omega_{m0}^{1/2}}{\max\,[(\Delta z_r/2z_r^{3/2}), (|z_a^{-1/2} - z_r^{-1/2}|)]} \, . \tag{4.9}$$

(If the comparison is made with an open, negatively curved universe rather than with an Einstein–de Sitter universe, M_a is enhanced. But for reasonable values of Ω_{m0} this effect is not substantial.)

Examples of evolution of the antipodal magnification of the MBR shell with epoch of observations are shown in Figure 3. We see that M_a varies considerably.

In the extreme case, if $|z_a - z_r| \lesssim \Delta z_r$, we would sit inside a real image of an MBR–emitting volume of linear size

$$\sim z_r \Delta l_r \approx 8\Omega_{m0}^{-1/2}h^{-1} \text{ Mpc} \, . \tag{4.10}$$

The angular magnification would then be $M_a \sim 800\Omega_{m0}^{1/2}$. The linear scale Δl_r, which is seen under $\Delta\theta_r(k \leq 0) \approx 8' \times \Omega_{m0}^{-1/2}$ (Kaiser and Silk 1986) in a flat or open universe, is then magnified to $\Delta\theta_r(|z_a - z_r| \leq \Delta z_r) \approx 100°$. The angular scales 4′ and 8°, investigated by Uson and Wilkinson (1984) and by Davies *et al.* (1987), respectively, would amount to fractions $\sim 7 \times 10^{-4}$ and ~ 0.08 of the MBR shell thickness, and the corresponding perturbations will be severely damped.

Let

$$\mathscr{D}(\theta) \equiv \langle(\delta T/T)^2\rangle^{1/2}(\theta) \tag{4.11}$$

be the observed temperature fluctuations, and let $\mathscr{D}_0(\theta)$ be the prediction for a flat or open universe, in some specific model of structure formation, in some specific observational setup. Then, in a universe with an antipode, we expect to observe

$$\mathscr{D}_a(\theta) = \mathscr{D}_0(\theta/M_a) \, . \tag{4.12}$$

Let us apply this general formula to a particular example. Bond and Efstathiou (1984) calculated $\mathscr{D}(\theta)$ for a three-beam experiment (e.g., Uson and Wilkinson 1984; Davies *et al* 1987) for the cold dark matter (CDM) model of structure formation. Their results (Fig. 1 and Table 1 in Bond and Efstathiou 1984) can be approximated by

$$\frac{\mathscr{D}_{\rm BE}(\theta)}{\mathscr{D}_{\rm BE}(\theta_c)} \approx \begin{cases} 1 & \text{for } \theta_c \le \theta \le \theta_h\,, \\ (\theta/\theta_c)^2 & \text{for } \theta < \theta_c\,, \end{cases} \quad (4.13)$$

where $\theta_c = \Delta\theta_r(k \le 0) \approx 8' \times \Omega_{m0}^{-1/2}$, and $10^{-5} < \mathscr{D}_{\rm BE}(\theta_c) < 10^{-4}$ for $0.2 \le \Omega_{m0} \le 1$. One horizon size is seen under an angle $\theta_h \approx 3° \times \Omega_{m0}^{-1/2}$.

In the "antipodal" cosmography we expect

$$\mathscr{D}_a(\theta) \approx 10^{-4} \begin{cases} 1 & \text{for } \theta \ge M_a \theta_c\,, \\ (\theta/M_a\theta_c)^2 & \text{for } \theta \le M_a\theta_c\,, \end{cases} \quad (4.14)$$

for an antipode at $z_a \ge 250$ (so that we can neglect the Sachs-Wolfe effect)., Setting, say, $z_a = 700$, we find $M_a\theta_c \approx 22°$, so that perturbations on 4′ and 8° would be reduced by factors $\sim 10^{-5}$ and $\sim 10^{-1}$, respectively.

On angular scales larger than $\Delta\theta_r = M_a\theta_c$, $\delta T/T$ is not affected by damping. In particular, for CDM with the Zel'dovich initial perturbation spectrum, the quadrupole anisotropy can be reduced by at most a factor $\sim \ln M_a$.

It is straightforward to apply the scaling to results obtained by other authors, e.g., by Wilson and Silk (1981) and by Gouda, Sasaki, and Suto (1987). The latter authors, in particular, presented a gauge-invariant treatment of density perturbations in a purely baryonic scenario. They predict $\mathscr{D}(\theta_c) \sim 10^{-3}$ to 10^{-4} for $0.1 < \Omega_{m0} < 1$. Taking our reduction effect into account, their conclusion that the Uson and Wilkinson (1984) bound on 4′ rules out scenarios with $\Omega_{m0} < 0.8$ is not applicable.

c) *Testing for High-z Antipodes*

Since the redshift thickness of the MBR shell, Δz_r, depends rather little on the cosmology (Jones and Wyse 1985), any measurement of its angular size, $\Delta\theta_r$, yields the angular diameter distance to the recombination shell. The coefficients of the Taylor expansion of the MBR brightness autocorrelation function, equation (4.7), can yield a rough estimate of $\Delta\theta_r$ from the ratios of two or more $C^{(n)}$, when measured. The proportionality coefficients in equation (4.7) depend on the cosmological details; however, a high-redshift antipode produces *anomalously large* $\Delta\theta_r$. Conversely, if the measured ratios between $C^{(n)}$ will not be anomalous, a large antipodal magnification will be ruled out.

A possible test can be a multibeam experiment on angular scales

$$\theta_c < \theta < \Delta\theta_r\,. \quad (4.15)$$

For instance, for $\theta \ll \Delta\theta_r$, triple-beam experiments with equidistant, aligned beams and signal summation $S_1 - 2S_2 + S_3$ measure

$$[\delta T/T]_{\rm triple} = (C^{(4)})^{1/2}\theta^2/2 \sim (\theta/\Delta\theta_r)^2\,,$$

whereas $[\delta T/T]_{\rm quintuple} \sim (\theta/\Delta\theta_r)^3$ can be measured in a quintuple-beam experiment with summation $S_1 - 4S_2 + 6S_3 - 4S_4 + S_5$. The ratio

$$R_{5/3} = [\delta T/T]_{\rm quintuple}/[\delta T/T]_{\rm triple}$$

must be small if $\theta \ll \Delta\theta_r$. This is in contrast to predictions of various theories for a flat universe with $\theta > \Delta\theta_r$; for instance, $R_{5/3} \sim 1$ for CDM with the Zel'dovich initial perturbation spectrum.

Another possible test, within particular theories of structure formation, can be obtained from comparison of the anisotropies at different angular scales.

We thus conclude: A high-redshift antipode can reduce the predictions for the apparent MBR anisotropy by a large factor, up to $6 \times 10^5\Omega_{m0}$, for $\theta \lesssim 10'$, for triple-beam experiments. The constraints on scenarios of structure formation obtained from the bounds on the MBR anisotropy are correspondingly weakened. The existence of a high-redshift antipode will be directly testable, when the MBR anisotropy (besides the dipole) will be discovered.

d) *An Antipode at a Moderately High Redshift*

We cannot exclude an antipode at $z > 5$. It may happen to lie within an object, say a forming galaxy or a cluster, which is sufficiently bright in a suitable wavelength range to produce a departure from the blackbody MBR spectrum (since the light of the source is nearly focused at us, it does not have to be exceptionally bright). In this case we would predict large dipole and higher multipole components for the departure (we sit inside the real image of an inhomogeneous source). Their axes can be misaligned with the MBR dipole and between themselves (for different multipoles).

V. EFFECTS OF GRAVITATIONAL LENSES

An ideally isotropic universe would focus our past light cone at our antipode (we trace the light rays backward). However, gravitational perturbations destroy the perfect focusing. The observed brightness distribution is thus distorted. In particular, brightness fluctuations originally on certain angular scales can be systematically transferred to smaller angular scales.

Blanchard and Schneider (1987) considered this effect in standard cosmographies, with respect to the usually expected MBR anisotropies. In this case, the MBR sky can be (almost) densely covered by regions affected in this way by galaxies, on the typical scale of a few arcseconds. Kashlinsky (1988) suggested an effect on the scale of a few arcminutes; however, this is excluded by observations (Cole and Efstathiou 1989; Kovner 1989).

If an antipode is near the microwave shell, lensing effects of all gravitational perturbations are enhanced by the antipodal magnification described in the last subsection. This enhancement is in fact the composite marginal lensing effect (see Kovner 1987). In particular, the constraint on maximal surface mass density of a perturbation necessary for multiple imaging becomes

$$\Sigma > \Sigma_{\rm min} \sim \Sigma_{\rm cr} = \frac{c^2}{4\pi G}\frac{d_{\rm os}}{d_{\rm ol}d_{\rm ls}} = 5 \times 10^{-4}\Omega_{m0}^{-1/2}h \text{ g cm}^{-2} \times \left(\frac{d_{\rm os}}{8\Omega_{m0}^{-1/2}h^{-1}\text{ kpc}}\right)\left(\frac{1h^{-1}\text{ Gpc}}{d_{\rm ol}}\right)\left(\frac{6h^{-1}\text{ Mpc}}{d_{\rm ls}}\right), \quad (5.1)$$

where $d_{\rm ol}$, $d_{\rm ls}$, and $d_{\rm os}$ are observer-lens, lens-source, and observer-source angular diameter distances.

Let us restrict our further analysis to the extreme case, $|z_a - z_r| \lesssim \Delta z_r$, and assume that $z_l \sim 1$ so that all the ratios in brackets in equation (5.1) are ~ 1. (In this case $\Sigma_{\rm min}$ is a factor ~ 1000 less than its typical value $\Sigma_{\rm min} \gtrsim 1$ g cm^{-2} in an Einstein–de Sitter universe. Typical galaxies probably have $\Sigma > \Sigma_{\rm min}$ in their cores.)

We simplify the analysis by drawing an analogy with the reflection of the Sun in an undulating water surface (Berry 1987 and references therein), rather than to calculate the complete correlation function of the temperature fluctuations. The analogy is legitimate, since on angular scales larger than at least $\gtrsim 1''$ the universe is not likely to be a substantially thick lens (a thin lens is equivalent to a mirror), for the following reason: a thick lens contains components at different distances from the observer; however, for our purpose, this is only important when background lens components can (or almost can) by multiply imaged by the foreground components. This does not happen on most of the sky (e.g., Kochanek and Apostolakis 1988; Kovner 1989 and references therein).

The image of the Sun in an undulating water surface is broken into many small images spread over directions within a cone of angular size $\sim\delta_{max}$, equal to the typical maximal deflection by waves (twice the slope of the water surface). Let us find the analogous δ_{max} in a loitering universe. It is important that the regions of deflection $\delta \lesssim \delta_{max}$ cover the sky densely, i.e., typically separated by $\delta_{sep} < \delta_{max}$.

The apparent deflection angle , δ, equal to the difference in angular positions of a point source and its image, can differ much from the actual deflection by a lens, $\Delta\theta$, since for a thin lens $\delta = (d_{ls}/d_{os})\Delta\theta$. For galaxies, in the singular isothermal sphere (SIS) approximation (Gott and Gunn 1974),

$$\delta = 4\pi\left(\frac{\sigma_l}{c}\right)^2 \frac{d_{ls}}{d_{os}} = 13' \times \Omega_{m0}^{1/2}\left(\frac{\sigma_l}{200\ \mathrm{km\ s^{-1}}}\right)^2 \times \left(\frac{d_{ls}}{6h^{-1}\ \mathrm{Mpc}}\right)\left(\frac{8\Omega_{m0}^{-1/2}h^{-1}\ \mathrm{kpc}}{d_{os}}\right), \quad (5.2)$$

where σ_l is the one-dimensional velocity dispersion (to compare, in an Einstein–de Sitter universe, $\delta \sim 1''$ for typical galaxies). This is larger than the conceivable range of validity of the SIS approximation (for a galaxy at $z \gtrsim 1$); however, typical projected separations between $\sigma_l \gtrsim 200$ km s^{-1} galaxies to redshift $z \sim 2$, are $\delta_{sep} \lesssim 10''$. Galaxies cannot be considered isolated, but within the range of dominance of a given galaxy it can be approximated by a SIS.

Cluster statistics is very uncertain. There may be $\sim 10^{4.5\pm1}$ clusters of $\sigma_l > 500$ km s^{-1} to redshift ~ 2 (Kovner 1987). We find $\delta \gtrsim 1°$ for SISs of such σ_l. The maximal random deflection available systematically over the whole sky thus lies in the interval

$$10' < \delta_{max} < 1° \quad (5.3)$$

and is determined by the mass associated with clusters of galaxies.

Let us now consider a patch of the MBR shell of brightness, say above the average background and of angular size $\theta < \delta_{max}$. Typically it is composed of many smaller images (the net flux in all the images is the same, on the average, as in the original). These images are spread over a solid angle $\Theta \gtrsim \delta_{max}$. The brightness contrast, for beam averaging on the scale θ, is thus reduced by a factor Θ^2/θ^2 (its gradient is reduced by Θ^3/θ^3); however, it is transferred to the scales of individual images.

The brightness contrast is thus transferred to the smaller angular scales "densely" available over the whole sky. However, the heterogeneity and clustering of galaxies would prevent complete transfer of the brightness contrasts to scales much smaller than a few arcseconds.

We conclude that the MBR brightness distribution on angular scales below δ_{max} can be affected by lenses. On the other hand, observation of δ_{max} can indicate the typical mass associated with clusters of galaxies. Lensing can thus further reduce the theoretical predictions for MBR anisotropies on the scale of a few arcminutes.

However, the expected MBR anisotropies on the scales 1′–1° in the extreme case of an antipode inside the MBR shell are already very small. Therefore, the lensing effects would be far below present-day sensitivity.

VI. CONCLUSIONS AND DISCUSSION

We find no contradictions with observations for an antipode at $z > 5$. It is marginally possible to have more than one antipode, if the nonrelativistic matter density is small, $0.01 < \Omega_{m0} < 0.03$. In this case, all antipodes except perhaps one are piled up at the redshift of extreme loitering. Loitering can stimulate the formation of galaxies at a certain redshift.

If an antipode at $z \sim 5$–10 happens to lie inside an object sufficiently bright in a suitable wavelength range, it may produce a departure from the blackbody spectrum of the MBR.

For $z_a \gtrsim 100$, our image of the MBR shell is magnified by a factor $10\Omega_{m0}^{1/2} \lesssim M_a \lesssim 800\Omega_{m0}^{1/2}$, and we observe damped anisotropies up to scales of 1°–90°. An antipode at redshift $z_a > 250$ would make us observe a causally connected MBR shell. Large magnifications are also possible in the case of an "almost antipode," i.e., $0 < \pi - \eta_0 \ll 1$. Thus more leeway is given to various cosmological scenarios which otherwise are severely constrained by the observed bounds on the MBR anisotropy.

Although anisotropies on scales up to $\sim 20°$ can be substantially reduced (§ III), the antipodal magnification effects on the quadrature anisotropies vary, for various mechanisms of structure formation. For instance, for the Zel'dovich initial perturbation spectrum and CDM, the quadrupole anisotropy can be reduced by at most a logarithmic factor $\sim \ln M_a$. In this case, the quadrupole limit $[\delta T/T]_q \le 3 \times 10^{-5}$ (Strukov, Skulachev, and Klypin 1988) imposes the most severe MBR–isotropy constraint.

The effect of brightness redistribution by gravitational lensing by galaxies and clusters is well below the present sensitivity of observations.

Superclusters and larger objects may have larger deflection angles; however, the regions affected by their effects may probably be confined to specific areas, rather than covering the sky densely. A spherical density fluctuation $\delta_\rho = \delta_\rho(3H^3/8\pi G)$ of radius R would shift a ray traced to the MBR shell by a maximal angle $\delta\theta = 2\delta_\rho(RH)^2$. The corresponding displacement at the MBR shell would be $\Delta l \sim 2\delta_\rho(RH)^2 d_{ls} \sim 13h^{-1}$ kpc $\times\, \delta_\rho(R/100h^{-1}\ \mathrm{Mpc})^2(H/H_0)^2(d_{ls}/6h^{-1}\ \mathrm{Mpc})$, possibly comparable to the shell thickness. A sufficiently large supercluster might thus destroy the causal connection of the observed MBR volume (if it could exist in the first place). But in this case the supercluster also might itself disturb the MBR to an observable degree (Rees and Sciama 1968).

We conclude that an antipode at high redshift can reduce theoretical expectations for MBR anisotropy well below what is usually inferred from structure formation scenarios. However, an antipode cannot explain the small degree of inhomogeneity of our universe at moderate redshifts.

A very precise tuning of the cosmological constant ($\Omega_{v0} \approx 1$) is required to make high-redshift antipodes possible. In this paper we do not propose any mechanism to produce the fine tuning; however, we note that little is known about the cosmological constant. Thus the notion of fine tuning may not necessarily be applicable.

There is some tuning in a different sense, namely, that the observed MBR isotropy depends on the cosmological time. In the past and in the future the angular magnification of the observed MBR shell can be very different.

Finally, we point out that a high-redshift antipode can be discovered or ruled out in a single multibeam experiment, or in any experiment that yields two or more coefficients of the Taylor expansion of the MBR autocorrelation function.

We thank R. W. Carswell, C. Hogan, A. Kashlinsky, A. Kassiola, N. Lazenby, M. Milgrom, B. Paczyński, M. J. Rees, J. Silk, A. Vilenkin, and S. D. M. White for enjoyable and valuable discussions, and the referee for a correction. Parts of this work were supported by SERC/RTA grant GR/E 51480, by the US–Israel Binational Scientific Foundation, and by the funds granted by the Charles H. Revson Foundation.

APPENDIX

Here we give some relations of interest.

I. INVERSION OF EQUATION (2.12)

For $\Omega_{m0} < 0.5$,

$$z_c = -1 + [\![\{\Omega_{m0}^{-1} - 1 + [\Omega_{m0}^{-1}(\Omega_{m0}^{-1} - 2)]^{1/2}\}^{1/3} + \{\Omega_{m0}^{-1} - 1 + [\Omega_{m0}^{-1}(\Omega_{m0}^{-1} - 2)]^{1/2}\}^{-1/3}]\!] . \tag{A1}$$

II. DECELERATION PARAMETER AND INFLECTION REDSHIFT

The deceleration parameter is

$$q = -\Omega_v + \Omega_m/2 = 1 - \ddot{a}a/\dot{a}^2 = \tfrac{1}{2}(1 - b\ddot{b}/\dot{b}) . \tag{A2}$$

It equals zero and changes sign at

$$z_i = (2\Omega_{v0}/\Omega_{m0})^{1/3} - 1 . \tag{A3}$$

The three redshifts z_i, z_c, z_m are always in the order

$$z_i \le z_c \le z_m . \tag{A4}$$

REFERENCES

Berry, M. V. 1987, *J. Opt. Soc. Am.*, **4**, 561.
Blanchard, A. 1984, *Astr. Ap.*, **132**, 359.
Blanchard, A., and Schneider, J. 1987, *Astr. Ap.*, **184**, 1.
Bond, J. R., and Efstathiou, G. 1984, *Ap. J. (Letters)*, **285**, L45.
Carswell, R. F., Webb, J. K., Baldwin, J. A., and Atwood, B. 1987, *Ap. J.*, **319**, 709.
Cole, S., and Efstathiou, G, 1989, *M.N.R.A.S.*, **239**, 195.
Davies, R. D. 1988, *Quart. J.R.A.S.*, **29**, 443.
Davies, R. D., Lasenby, A. N., Watson, R. A., Daintree, E. J., Hopkins, J., Beckman, J., Sanchez-Almeida, J., and Rebolo, R. 1987, *Nature*, **326**, 462.
Durrer, R., and Straumann, N. 1990, *M.N.R.A.S.*, **242**, 221.
Efstathiou, G., and Bond, R. 1987, *M.N.R.A.S.*, **227**, 33P.
Ehlers, J., and Rindler, W. 1989, *M.N.R.A.S.*, **238**, 503.
Gott, J. R. 1985, in *IAU Symposium 117, Dark Matter in the Universe*, ed. G. Knapp and J. Kormendy (Dordrecht: Reidel), p. 119.
Gott, J. R., and Gunn, J. E. 1974, *Ap. J. (Letters)*, **190**, L105.
Gott, J. R., Park, M. G., and Lee, H. M. 1989, *Ap. J.*, **338**, 1.
Gott, J. R., and Rees, M. J. 1987, *M.N.R.A.S.*, **227**, 453.
Gouda, N., Sasaki, M., and Suto, Y. 1987, *Ap. J. (Letters)*, **321**, L1.
Hewitt, A., and Burbidge, G. 1987, *Ap. J. Suppl.*, **63**, 1.
Jones, B. J. T., and Wyse, F. G. 1985, *Astr. Ap.*, **149**, 144.
Kaiser, N. 1984, *Ap. J.*, **282**, 374.
Kaiser, N., and Silk, J. 1986, *Nature*, **324**, 529.
Kashlinsky, A. 1988, *Ap. J. (Letters)*, **331**, L1.
Kochanek, C. S., and Apostolakis, J. 1988, *M.N.R.A.S.*, **235**, 1073.
Kovner, I. 1987, *Ap. J.*, **321**, 686.
———. 1989, in press.
Kovner, I., and Rees, M. J. 1989, *Ap. J.*, **345**, 52.
Occhionero, F., Vittorio, N., Carnevali, P., and Santangelo, P. 1980, *Astr. Ap.*, **86**, 212.
Peebles, P. J. E. 1980, *The Large Scale Structure of the Universe* (Princeton: Princeton University Press).
Petrosian, V., Salpeter, E., and Szekeres, P. 1967, *Ap. J.*, **147**, 1222.
Rees, M. J., and Sciama, D. W. 1968, *Nature*, **217**, 511.
Rowan-Robinson, M. 1968, *M.N.R.A.S.*, **141**, 445.
Sachs, R. K., and Wolfe, A. M. 1967, *Ap. J.*, **147**, 73.
Shklovsky, I. 1967, *Ap. J. (Letters)*, **150**, L1.
Silk, J., and Vittorio, N. 1987, *Ap. J.*, **317**, 564.
Strukov, I. A., Skulachev, D. P., and Klypin, A. A. 1988, in *IAU Symposium 130, Large Scale Structures of the Universe*, ed. J. Audouze, M.-C. Pelletan, and A. Szalay (Dordrecht: Kluwer), p. 27.
Trimble, V. 1987, *Ann. Rev. Astr., Ap.*, **25**, 425.
Uson, J., and Wilkinson, D. T. 1984, *Nature*, **312**, 427.
Webb, J. K., Parnell, H. C., Carswell, R. F., McMahon, R. G., Irwin, M. J., Hazard, C., Ferlet, R., and Vidal-Madjar, A. 1988, *Messenger*, **15**, 15.
Weinberg, S. 1989, *Rev. Mod. Phys.*, **61**, 1.
Wilson, W. L., and Silk, J. 1981, *Ap. J.*, **243**, 14.
Zel'dovich, Ya. B., and Sunyaev, R. A. 1969, *Ap. Space Sci.*, **4**, 301.

RUTH DURRER: Physics Department, Princeton University, Princeton, NJ 08544

ISRAEL KOVNER: Physics Department, Weizmann Institute, Rehovot 76100, Israel (offprint requests).